Controllable Binding of Polar Molecules and Metastability of One-Dimensional Gases with Attractive Dipole Forces

Jason N. Byrd,* John A. Montgomery, Jr., and Robin Côté

Department of Physics, University of Connecticut, Storrs, Connecticut 06269, USA
(Received 7 November 2011; published 24 August 2012)

We explore one-dimensional samples of ultracold polar molecules with attractive dipole-dipole interactions and show the existence of a repulsive barrier caused by a strong quadrupole interaction between molecules. This barrier can stabilize a gas of ultracold KRb molecules and even lead to long-range wells supporting bound states between the molecules. The properties of these wells can be controlled by external electric fields, allowing the formation of long polymerlike chains of KRb and studies of quantum phase transitions by varying the effective interaction between molecules. We discuss the generalization of those results to other systems.

Recent achievements in the formation and manipulation of ultracold polar molecules [1,2] have opened the gate to exciting new studies in several fields of physical sciences. Polar molecules could find uses in quantum information [3] and precision measurements [4], while their long-range and anisotropic interactions in dense samples could provide a fertile ground for novel quantum gases [5]. In addition, advances in controlling the alignment and orientation of polar molecules [6,7] enable the manipulation of these inter-molecular interactions, building a bridge between atomic, molecular, and optical physics, physical chemistry, and condensed matter physics. Until now, stable dipolar gases were thought to require a repulsive dipole-dipole interaction, such as provided by parallel dipoles perpendicular to a two-dimensional plane. However, to observe interesting new correlations and phases, such as the Luttinger liquid transition [8], attractive interactions are needed. In this Letter, we propose and investigate a system with such features, combining the available techniques to produce ultracold polar molecules with the ability to precisely control their orientation.

In this study, we focus on KRb, which has been trapped in relatively large amounts [1]. We first calculate the potential energy surface (PES) $V(R, \theta_1, \theta_2, \phi)$ of two KRb molecules approaching each other for a wide range of geometries. We assume that both the molecules are in the ro-vibrational ground state of their electronic $X^1\Sigma^+$ ground state, with rigid rotors, an approximation that is valid for $R \sim 20$ a.u. or larger. Figure 1 shows the PES for three particular geometries when both the molecular axes are in the same plane ($\phi = 0$): the top, middle, and bottom panels depict V when the molecules are aligned ($\theta_1 = \theta_2 = 90°$), in the T-orientation ($\theta_1 = 0$, $\theta_2 = 90°$), and collinear ($\theta_1 = \theta_2 = 0$), respectively. Those curves illustrate the difference between the stronger short-range region, where the electronic wave function becomes perturbed, and the weaker long-range region, where the bond length of each KRb is not affected. The short-range region is generally deep and strongly angular dependent, with

wells ranging from a few 100 K, as in Fig. 1 for co-planar geometries, to the tetramer K_2Rb_2 bound by ~ 4300 K with respect to the KRb + KRb threshold [9,10]. The KRb + KRb PES was calculated at the coupled cluster theory including all singles, doubles, and perturbative triples using MOLPRO 2009.1 [11,12], with the K and Rb core electrons replaced by the Stuttgart relativistic ECP18SDF [13] and ECP36SDF [14] pseudopotentials, respectively. The core-valence correlation energy was modeled using a core polarization potential [13]. Supplemental basis functions were added to existing uncontracted basis sets for K [15] and Rb [16]. The exponents were optimized to reproduce the experimental equilibrium bond length, R_e, and dissociation energy, D_e [17].

Our analysis is concentrated on the coplanar geometries of Fig. 1, which depicts a seemingly surprising result.
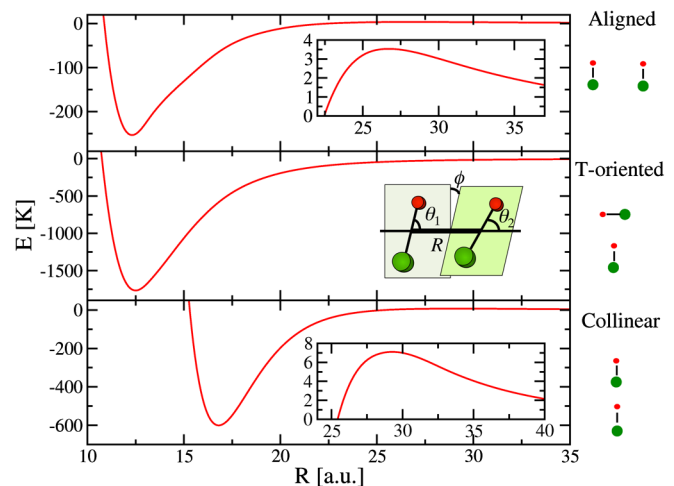

FIG. 1 (color online). KRb + KRb PES for coplanar geometries: aligned (top), T-oriented (middle), and collinear (bottom). The inset sketches the geometry: **R** joins the geometric center, two KRbs θ_1 and θ_2 are the angles between their molecular axes and **R**, and ϕ is the angle between the molecular planes.

While the top and middle panels depict the expected behavior of a repulsive and slightly attractive dipole-dipole interaction, respectively, the collinear geometry (bottom panel) reveals a barrier. The existence of this barrier can be traced to a strong repulsive quadrupole interaction. We also notice that it is higher (almost 7 K in height) than that of the aligned geometry (about 4 K). To better understand these *ab initio* results, we examine the KRb + KRb interaction in the long-range region where the intermolecular wave function overlap is negligible and the interaction can be expressed by the long-range expansion

$$V(R, \theta_1, \theta_2, \phi) \overset{R \text{ large}}{=} -\sum_n \frac{W_n(\theta_1, \theta_2, \phi)}{R^n}. \quad (1)$$

The functions W_n may contain electrostatic (e.g., dipole $\mathcal{D}$, quadrupole $\mathcal{Q}$, octupole $\mathcal{O}$, etc.) and/or dispersion and induction contributions $C_{n,i}$ [18,19]. The first few terms are

$$W_3 = \mathcal{D}^2(2c_1c_2 - s_1s_2c_\phi),$$

$$W_4 = \frac{3\mathcal{D}\mathcal{Q}}{2}(1 + 3c_1c_2 - 2s_1s_2c_\phi)(c_1 - c_2),$$

$$W_5 = \mathcal{D}\mathcal{O}\left\{\frac{3}{2}s_1s_2c_\phi(2 - 5c_1^2 - 5c_2^2) - c_1c_2(6 - 5c_1^2 - 5c_2^2)\right\} - \mathcal{Q}^2\left\{\frac{3}{2}(1 - 3c_1^2)(1 - 3c_2^2) - 12c_1c_2s_1s_2c_\phi + \frac{3}{4}s_1^2s_2^2c_{2\phi}\right\},$$

$$W_6 = C_{6,0} + C_{6,1}(3c_1^2 + 3c_2^2 - 2) + C_{6,2}(3c_1^2 - 1)(3c_2^2 - 1) + C_{6,3}c_1c_2s_1s_2c_\phi + C_{6,4}s_1^2s_2^2c_{2\phi},$$

where $c_i \equiv \cos\theta_i$, $s_i \equiv \sin\theta_i$, and $c_{k\phi} \equiv \cos k\phi$. In Table I, we list the corresponding parameters obtained by least squares fit of the PES up to $n = 8$. The fitted $\mathcal{D}$, $\mathcal{Q}$, and $\mathcal{O}$ are also compared to the *ab initio* values calculated at the all-electron coupled-cluster single double level of theory with the Roos atomic natural orbital basis set [20]. $\mathcal{D}$ and $\mathcal{Q}$ agree to better than 1%, attesting to the accuracy of the PES, while $\mathcal{O}$ is off by one order of magnitude, reflecting the small contribution of $\mathcal{D}\mathcal{O}$ in W_5. Using Eq. (1), one can understand the physical origin of the barriers. For parallel molecules, i.e., $\theta_1 = \theta_2 \equiv \theta$ and $\phi = 0$, the two leading terms in V are

$$V(R, \theta) \simeq -\frac{W_3}{R^3} - \frac{W_5}{R^5}. \quad (2)$$

For collinear KRb, $\theta = 0$, with $W_3 = 2\mathcal{D}^2$ and $W_5 = -6\mathcal{Q}^2 + 4\mathcal{D}\mathcal{O} \simeq -6\mathcal{Q}^2$, and because of the relatively weak $\mathcal{D}$ when compared to $\mathcal{Q}$, the long-range attractive R^{-3} dipole interaction is overcome by a shorter-range repulsive R^{-5} quadrupole interaction (the attractive contribution of $\mathcal{D}\mathcal{O}$ is much weaker than that of the repulsive $\mathcal{Q}^2$); still, at a shorter range, the attractive R^{-6} and higher contributions dominate and bring V down, and hence the barrier. For aligned KRb, $\theta = 90°$, with $W_3 = -\mathcal{D}^2$ and $W_5 = -(9/4)\mathcal{Q}^2 + 3\mathcal{D}\mathcal{O} \simeq -(9/4)\mathcal{Q}^2$, and the leading repulsive W_5 is about three times smaller than for the collinear case, and hence the smaller barrier shown in Fig. 1.

Using Eq. (1), we study the geometries leading to the long-range barrier; Figure 2 depicts its height V_{top} as a function of θ_1 and θ_2 for a few twist angles ϕ. For $\phi = 0$, a substantial barrier exists along the diagonal $\theta \equiv \theta_1 = \theta_2$ for small angles ($\theta \sim 20°$ or less) and for large angles ($\theta \sim 70°$ or more). While the barrier remains present for a small angle cone ($\sim 20°$) as ϕ increases, it quickly disappears for a large θ. Roughly speaking, there is a barrier for a cone of $\theta \sim 20°$ for any ϕ, and for a larger molecular misalignment, the barrier vanishes. A significant barrier can thus be maintained by aligning the molecules within a small angular cone, allowing ultracold KRb samples to remain stable and even be evaporatively cooled in various trap geometries (one dimensional when nearly collinear, and one or two dimensional when nearly aligned).

Polar molecules can be oriented by coupling rotational states along a polarizing external electric field **F**. This can

TABLE I. Left: fit parameters (up to R^{-6}). Right: *ab initio* values of the equilibrium separation R_e, moments $\mathcal{D}$, $\mathcal{Q}$, and $\mathcal{O}$ (from the geometric center), collinear orientation W_6, and the turning points R_{sr} and $R_\mathcal{Q}$ for various molecules AB in $v = 0$ of $X^1\Sigma^+$. All values are in atomic units.

KRb fit		AB	R_e	$\mathcal{D}$	$\mathcal{Q}$	$\mathcal{O}$	W_6	R_{sr}	$R_\mathcal{Q}$
$\mathcal{D}$	0.234	KRb	7.69	0.234	16.99	−3.16	18,528	10.7	126
$\mathcal{Q}$	17.06	LiNa	5.45	0.246	10.56	−1.80	4,265	6.34	74.4
$\mathcal{O}$	−23.71								
$C_{6,0}$	11679	RbCs	8.37	0.554	14.19	−5.39	26,599	21.6	44.6
$C_{6,1}$	3182								
$C_{6,2}$	10441	LiRb	6.50	1.715	11.80	−1.61	8,528	9.95	12.0
$C_{6,3}$	−2893	LiCs	6.93	2.335	11.00	−7.26	10,951	12.7	8.5
$C_{6,4}$	158	NaK	6.61	1.199	12.91	3.83	9166	9.52	18.5
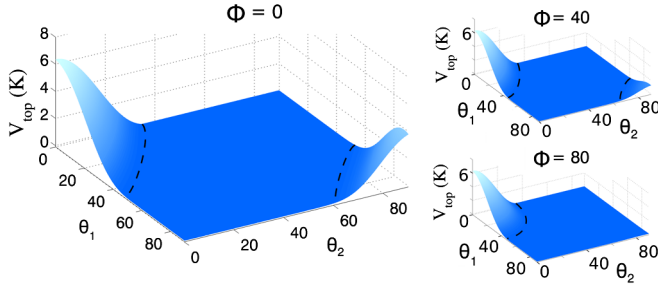
FIG. 2 (color online). V_{top} vs θ_1 and θ_2. The main plot corresponds to a twist angle $\phi = 0$, while the two smaller plots to $\phi = 40°$ (top) and $80°$ (bottom). V_{top} is set to zero if there is no barrier.
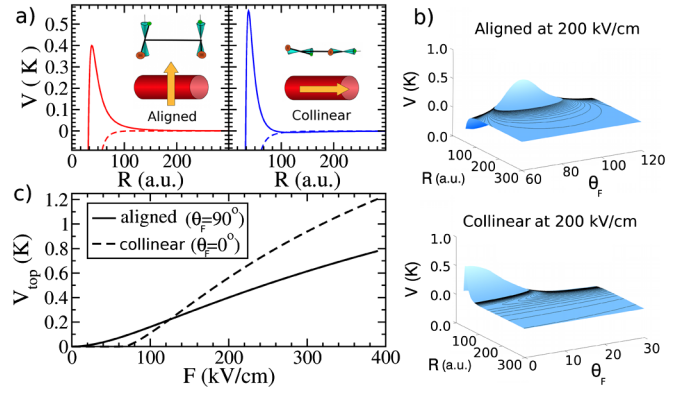

FIG. 3 (color online). (a) KRb + KRb interaction (one dimensional) for weak (5 kV/cm: dashed lines) and strong electric fields (200 kV/cm: solid lines), for aligned (left) and collinear (right) orientations. The red cylinder represents the one-dimensional trap, the arrow the orientation of the field, and the sketch above the precessing molecules. (b) Intermolecular interaction with $F = 200$ kV/cm for the aligned (top) and collinear (bottom) geometries as a function of θ_F. (c) Height of the barrier for aligned and collinear orientations as a function of F.

be achieved by using a dc electric field; however, the small dipole moment of KRb requires field strengths that are difficult to achieve in the laboratory. An alternative is to add a separate polarizing laser field [21] that directly couples the rotational states of the molecule. Although this utilizes a much smaller dc field, nonadiabatic effects are prominent [6], and for the sake of simplicity, we calculate the rotational state coupling by increasing the dc external field. We start with a superposition of field-free symmetric top states

$$|\tilde{J}\tilde{M}\,\Omega\rangle = \sum_{J,M} a_{M,\tilde{M}}^{J,\tilde{J}} |JM\Omega\rangle, \qquad (3)$$

labeled by their total angular momentum J with projection M along $\mathbf{F}$. After transforming the molecule-fixed frame potential $V(R, \theta_1, \theta_2, \phi)$ to the laboratory-fixed frame $V_{\text{Lab}}(\mathbf{R}, \hat{r}_1, \hat{r}_2)$ [22], the field averaged potential is found by evaluating

$$V(\mathbf{R}) = \langle \tilde{J}'\tilde{M}'\Omega' | V_{\text{Lab}}(\mathbf{R}, \hat{r}_1, \hat{r}_2) | \tilde{J}\tilde{M}\,\Omega\rangle. \qquad (4)$$

In Fig. 3, we illustrate the effect of $\mathbf{F}$ on a pair of KRb molecules in one dimension, with θ_F defined as the angle between $\mathbf{F}$ and $\mathbf{R}$. For weak fields ($F \lesssim 10$ kV/cm), the molecules remain largely in the first two ($J = 0, 1$) rotational states. Classically, they precess "wildly" on a wide cone about $\mathbf{F}$ averaging over a large range of relative angles, with the dominant contribution coming from the isotropic $C_{n,0}$ terms. This is depicted by the dashed lines in Fig. 3(a) for two orientations. In both cases, the interaction becomes strongly attractive at short distance, with the aligned geometry having a weak barrier (~ 1 mK) and the collinear case showing no sign of a barrier. The solid lines show the effect of a larger electric field where $\mathbf{F}$ strongly mixes more (~ 7) J's and strong barriers are present for both illustrated orientations. Figure 3(b) shows the tightly aligned interaction for a range of θ_F near the aligned and collinear orientations, where we obtain results similar to those in the molecular frame. The barrier survives for a cone of angle θ_F of about $20°$ for both orientations, and the same conclusions about stability of one-dimensional and two-dimensional samples apply.

For the aligned orientation, the barrier appears rapidly even for low fields, while larger fields ($F \gtrsim 70$ kV/cm) are necessary for the collinear case [see Fig. 3(c)]. In both cases, the barrier grows rapidly to hundreds of mK, a value much higher than the typical kinetic energy of the trapped ultracold molecules (< 100 μK).

Figure 3(b) hints at the existence of a long-range well for the collinear geometry. We analyze this well in the molecular frame when the molecules are fully parallel ($\theta \equiv \theta_1 = \theta_2$ and $\phi = 0$). We find a long-range well with several bound levels caused by its breadth and the large mass of the KRb molecules. For $\theta = 0$, there are seven levels, the deepest bound by ~ 2.7 mK, with classical turning points at 110 and 205 a.u. As θ increases, the R^{-5} repulsion gets smaller and the well deepens, and the binding energies increase proportionately until θ reaches $\theta_c \simeq 22°$, at which point the barrier disappears [see Fig. 4(a)]. We note that for a small deviation from $\theta = 0$, the binding energies are not significantly affected, and an additional level $\nu = 7$ appears for $18° < \theta < \theta_c$ [inset in Fig. 4(a)].

The variation of bound levels with θ affects the scattering between molecules and their effective interaction. Assuming θ (or θ_F) as a fixed external parameter, we estimate the s-wave scattering phase shift δ between two KRb molecules, which depends on the interaction V and wave number k; $\delta < 0 (> 0)$ corresponds to an effective repulsive (attractive) interaction. Here, we choose k assuming $\hbar^2 k^2 \sim m k_B T$ (m: mass of KRb; k_B: Boltzmann constant) for $T \simeq 700$ nK [1] and illustrate the effect in Fig. 4(b) in the molecule frame. For small angles ($\theta \lesssim 14.7°$), the interaction is attractive (with $\delta > 0$), while it becomes repulsive ($\delta < 0$) for larger angles. In an ideal one-dimensional trap, the repulsive barrier at $R \sim 100$ a.u. would stabilize the sample for
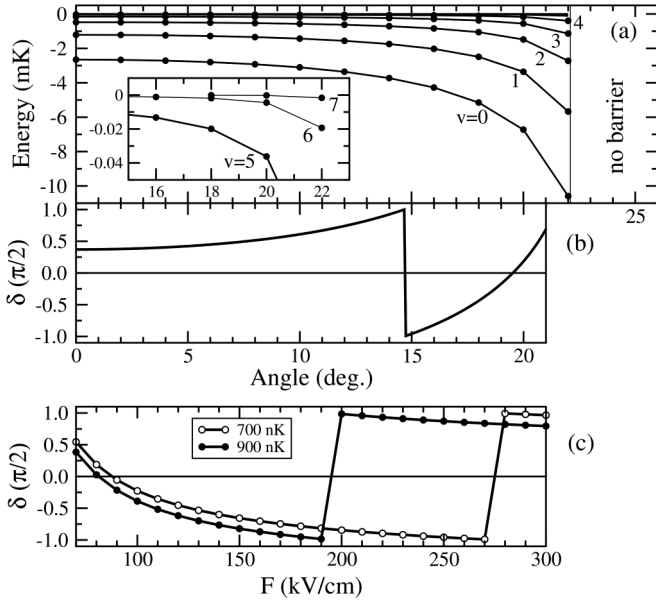
FIG. 4. (a) Long-range well energy levels vs θ; an additional level $v = 7$ appears at $18°$ (inset). (b) Scattering phase shift δ vs θ for k corresponding to 900 nK for infinite F. (c) δ as a function of the field strength F for $\theta_F = 0$ at collision energies corresponding to 700 and 900 nK.

an attractive effective interaction by preventing the molecules from reaching short distances where inelastic processes could take place. Larger angles would also give stable samples since the effective interaction is repulsive. By varying the orientation of the electric field with respect to the trap axis, the behavior of the sample could be controlled; an effective attractive interaction would lead to a dense self-trapped system, i.e., a liquidlike sample, while an effective repulsive interaction would give a dilute sample behaving like a gas. Such control could probe a quantum phase transition between a Luttinger liquid and an ultracold gas [8]. One could also create a chain of KRb molecules weakly bound together (e.g., by using photoassociation); these would be akin to ultracold polymerlike chains stabilized by an external electric field and a one-dimensional trap. We note that the effective interaction can also be controlled by varying the magnitude of **F**. In Fig. 4(c), we show δ for $\theta_F = 0$ as a function of F for two collision energies corresponding to 700 and 900 nK, and find that its sign can be changed by varying F.

Obtaining one-dimensional traps is a challenging task; assuming a harmonic trap in the perpendicular direction characterized by the frequency ω, the size of the ground state $a \sim \sqrt{\hbar/m\omega}$ is of the order of a few 1000 a.u. for optical traps. Molecules at densities of 10^{12} cm^{-3} loaded in such traps would be separated by roughly $d \sim 1$ μm, and for repulsive effective interaction, the angle $\tan^{-1} a/d \lesssim 10°$ between their axes would remain within the cone of stability. For an attractive effective interaction, the relevant angle is $\tan^{-1} a/R_Q$, where R_Q is the point

where the barrier begins for two approaching molecules, which requires $a \sim 0.4 R_Q = 50$ a.u. for KRb. Here, the sample would not be one dimensional and inelastic processes would not be allowed. Nonreactive species, such as RbCs, could be considered to prevent inelastic processes, or much tighter magnetic traps could be employed, in which case, molecules in a triplet electronic state with a magnetic moment μ would be required. For KRb in its a $^3\Sigma^+(v = 0)$ state, $a \sim 60$ a.u. can be achieved [23], and with $R_Q \sim 150$ a.u. [24], $\tan^{-1} a/R_Q$ would remain within the stability cone.

The features discussed here for KRb can be generalized to other polar molecules. The existence of a barrier for perfectly collinear molecules depends mostly on the first two terms of Eq. (1) [see Eq. (2)]. By setting $V = 0$ and overlooking $\mathcal{DO}$, we find $R_Q \simeq \sqrt{3\mathcal{Q}^2/\mathcal{D}^2}$, the point where the R^{-5} repulsion takes over R^{-3} attraction. We can also define a point R_{sr} where a shorter range R^{-6} attraction takes over R^{-5} repulsion, and by overlooking the other contributions, we can obtain $R_{sr} = -W_6/W_5$. If R_Q is outside the region where the bonds are strongly perturbed or higher W_n terms do not contribute significantly ($R_{sr} < R_Q \lesssim 20$ a.u.), then the barrier may exist. Table I gives R_Q and R_{sr} for various polar molecules. Due to its large variance, $\mathcal{D}$ dictates the R_Q behavior of the systems. Molecules with a small $\mathcal{D}$ (e.g., LiNa and KRb) have a sizable R_Q, and so the existence of a barrier is very likely, unlike in those with a large $\mathcal{D}$ (e.g., LiRb, LiCs, and NaK). We also include RbCs, for which the existence of a barrier is uncertain. This is interesting since RbCs are known to be nonreactive.

In conclusion, we found that the interaction between polar molecules exhibits a strong barrier when they are oriented about two specific geometries, aligned and collinear. We also showed that the collinear setting gives meta-stable samples of ultracold molecules in a tight one-dimensional trap. Long-range R^{-3} dipolar attractive and R^{-5} quadrupolar repulsive contributions in the collinear geometry lead to long-range wells between polar molecules, sustaining several bound levels. Varying the orientation of the molecules using an external electric field allows for nontrivial effects, such as changing the effective interaction from repulsive to attractive, and possibly the phase of the sample from gas to liquid. Finally, we also predict the existence of a collinear barrier for various bi-alkali polar molecules based on the relative strength of the dipole and quadrupole moments. A combination of the available techniques to produce ultracold molecules [1,2] and the ability to precisely control their spatial orientation [6,7] provide the tools to investigate such systems.

*byrd@phys.uconn.edu

[1] M. de Miranda, A. Chotia, B. Neyenhuis, D. Wang, G. Quéméner, S. Ospelkaus, J. Bohn, J. Ye, and D. Jin, Nature Phys. **7,** 502 (2011).

[2] J. Deiglmayr, M. Repp, R. Wester, O. Dulieu, and M. Weidemüller, Phys. Chem. Chem. Phys. **13,** 19101 (2011).

[3] S. F. Yelin, K. Kirby, and R. Côté, Phys. Rev. A **74,** 050301(R) (2006).

[4] D. DeMille, F. Bay, S. Bickman, D. Kawall, D. Krause, S. E. Maxwell, and L. R. Hunter, Phys. Rev. A **61,** 052507 (2000).

[5] L. Santos, G. V. Shlyapnikov, P. Zoller, and M. Lewenstein, Phys. Rev. Lett. **85,** 1791 (2000).

[6] J. H. Nielsen, H. Stapelfeldt, J. Küpper, B. Friedrich, J. J. Omiste, and R. González-Férez, Phys. Rev. Lett. **108,** 193001 (2012).

[7] L. Holmegaard, J. H. Nielsen, I. Nevo, H. Stapelfeldt, F. Filsinger, J. Kupper, and G. Meijer, Phys. Rev. Lett. **102,** 023001 (2009).

[8] A. Recati, P. O. Fedichev, W. Zwerger, and P. Zoller, Phys. Rev. Lett. **90,** 020401 (2003).

[9] J. N. Byrd, J. A. Montgomery, Jr., and R. Côté, Phys. Rev. A **82,** 010502(R) (2010).

[10] J. N. Byrd, H. H. Michels, J. A. Montgomery, Jr., R. Côté, and W. C. Stwalley, J. Chem. Phys. **136,** 014306 (2012).

[11] H. J. Werner, P. J. Knowles, R. Lindh, F. R. Manby, and M. Schütz *et al.*, Molpro, version 2009.1, a package of *ab initio* programs, (2009).

[12] P. J. Knowles, C. Hampel, and H. J. Werner, J. Chem. Phys. **99,** 5219 (1993).

[13] P. Fuentealba, H. Preuss, H. Stoll, and L. V. Szentpály, Chem. Phys. Lett. **89,** 418 (1982).

[14] P. Fuentealba, H. Stoll, L. v. Szentpaly, P. Schwerdtfeger, and H. Preuss, J. Phys. B **16,** L323 (1983).

[15] S. Magnier and P. Millie, Phys. Rev. A **54,** 204 (1996).

[16] M. Aymar and O. Dulieu, J. Chem. Phys. **122,** 204302 (2005).

[17] A. Pashov, O. Docenko, M. Tamanis, R. Ferber, H. Knöckel, and E. Tiemann, Phys. Rev. A **76,** 022511 (2007).

[18] F. Mulder, A. van der Avoird, and P. E. S. Wormer, Mol. Phys. **37,** 159 (1979).

[19] J. N. Byrd, R. Côté, and J. A. Montgomery, Jr., J. Chem. Phys. **135,** 244307 (2011).

[20] B. Roos, V. Veryazov, and P.-O. Widmark, Theor. Chem. Acc. **111,** 345 2004.

[21] M. Härtelt and B. Friedrich, J. Chem. Phys. **128,** 224313 (2008).

[22] T. V. Tscherbul, Y. V. Suleimanov, V. Aquilanti, and R. V. Krems, New J. Phys. **11,** 055021 (2009).

[23] R. Folman, P. Krüger, J. Schmiedmayer, J. Denschlag, and C. Henkel, Adv. At. Mol. Opt. Phys. **48,** 263 (2002).

[24] $\mathcal{D} = 0.017$ a.u. and $\mathcal{Q} = 1.47$ a.u. were computed consistently with the other methods in the text.